A Dual Frequency Antenna for RSSI-based DOA Estimation - from Theory to Prototype

Hartmann M.

Friedrich-Alexander-Universität Erlangen-Nürnberg (FAU), InformationTechnologies, 91058 Erlangen, Germany; e-mail: markus.hartmann@fau.de

Wohler M., Schühler M. and Weisgerber L.

Fraunhofer Institute for Integrated Circuits (IIS), 91058 Erlangen, Germany

Thielecke J. and Heuberger A.

Friedrich-Alexander-Universität Erlangen-Nürnberg (FAU), InformationTechnologies, 91058 Erlangen, Germany

Wildlife monitoring, e.g. tracking bats, is one of many emerging applications applying wireless sensor networks. In this paper, a dual band antenna for field strength-based direction finding is presented. The complete design process including theoretical considerations and simulations towards a working prototype is shown. To meet the networks crucial requirements of robustness and low-cost fabrication the design of the antenna pursues a passive approach to realize a set of two orthogonal radiation patterns without side-lobes. The antenna is influenced by the small element separation, i.e. additional side-lobes and impedance transformation. The effects are compensated by an optimized element arrangement, as well as a dual-band matching and decoupling of the antenna elements. The proposed directional antenna array provides a gain pattern suitable for precise field strength-based direction of arrival estimation.

1 Introduction

Wireless sensor networks (WSN) are getting more and more into focus of research in a wide area of applications. One of these is the behavioral studies in biology applying WSN. In [1] a WSN is presented to analyze habitat selection of seabirds. In [2] a WSN is shown equipping bats with wireless sensor nodes (SNs) for encounter detection to study the social interactions between multiple individuals. Similarly, we localize the flight trajectory of bats, as depicted in Figure 1, by multiple stationary SNs. The direction of arrival (DOA) of the bat signal is estimated by multiple SNs. The position of the bat is estimated by simple triangulation or more sophisticated algorithms as presented in [3]. The optimal antenna pattern shape for received signal strength (RSS)-based DOA estimation in a certain base station arrangement is investigated in [4] and can be characterized by an eight-like shape. A main challenge for radio frequency (RF) localization is multi-path propagation, which leads to fading and DOA estimation errors. This major issue is addressed by adding additional redundancy using two separate frequency bands. The presented paper covers the design process of a RSS-DOA antenna for dual-band operation.

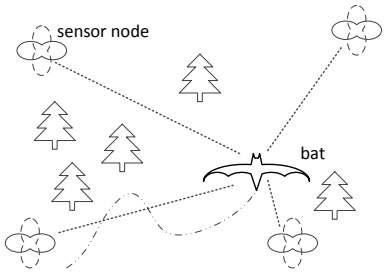

Figure 1: Localization principle for tracking bats applying DOA measurements from four sensor nodes (SN). DOA estimation bases on field strength difference measurements with two different antenna patterns per SN (solid antenna pattern and dashed pattern)

The design aims at a low-cost prototype antenna, providing the suitable characteristics for RSS-DOA estimation. In Section II the fundamentals of field strength-based DOA estimation are discussed. In Section III an advanced method for antenna pattern shaping is shown. Section IV shows the implementation of the antenna, which mainly focusses on the decoupling of elements for both operating frequency bands. Furthermore, it compares the results obtained from analytic calculations with the ones from numeric simulations and measurement. Section V concludes this paper.

2 Field Strength-based DOA Estimation

The RSS-DOA estimation is implemented by field strength difference measurements of different antennas or antenna beams. In [5] a switched-beam antenna for RSS-DOA estimation is presented. In [4] a similar ap-

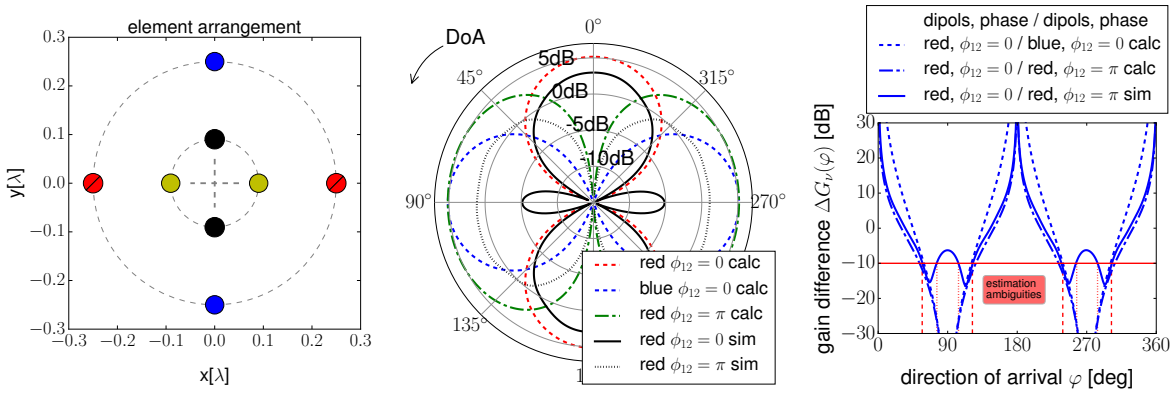

(a) (b) (c)

Figure 2: Subfigure (a) shows the spatial distribution for a dual frequency array with two elements for each pattern with a distance of $0.5\lambda_0$ between the elements for 868 MHz and 2.4 GHz. The resulting directivity pattern for different feedings ($\phi_{12} = 0$ and $\phi_{12} = \pi$) and dipole arrangements is shown in Subfigure (b). Additionally the calculated and simulated antenna pattern for 868 MHz including side-lobes caused by coupling to the 2.4 GHz antenna elements is presented. Subfigure (c) represents the resulting gain difference function $\Delta G_\nu(\varphi)$ for 868 MHz.

proach with a fixed pattern antenna is shown, where the shapes of the antenna pattern are optimized for a best possible DOA estimation. Basically, the received field strength difference ΔP_{RX} in dB of two directional antennas can be described by:

$$\Delta P_{\mathrm{RX}} = G_{\mathrm{RX},1}(\varphi) - G_{\mathrm{RX},2}(\varphi) := \Delta G_\nu(\varphi), \quad (1)$$

where φ is the DOA. $G_{\mathrm{RX},1}$ and $G_{\mathrm{RX},2}$ are the gain functions in dB of the antenna with respect to the DOA φ. The antenna patterns from Figure 2b for $G_{\mathrm{RX},1}$ and $G_{\mathrm{RX},2}$ are represented by the dashed lines, the gain difference function $\Delta G_\nu(\varphi)$ is shown in Figure 2c by the dashed line. This is equivalent to the measured ΔP_{RX} in an environment with low multi-path effects. The DOA of the electromagnetic wave is estimated with some ambiguities as shown in Fig. 2c. For a certain gain difference value ΔG_ν multiple DOAs φ are valid. The number of lobes, even side-lobes, directly influences the ambiguity of the estimation and has to be solved by localization algorithms. A higher level of ambiguity, especially caused by side-lobes, drastically degrades the localization accuracy.

3 Antenna Pattern Synthesizing

As already discussed in [4] a fixed beam antenna pattern is formed by multiple antenna elements and the geometrical arrangement of these antenna elements. In contrast to [5] a completely passive approach without any beam switching is prefered due to the use of short burst signals. In [4] an optimized shape of the antenna pattern is presented, featuring its geometrical arrangement of multiple elements, for the purpose of RSS-based DOA estimation.

To describe the radiation pattern originating from an array of antenna elements, the array factor [6] is defined by

$$AF = \sum_{i=0}^{n-1} w_i e^{-j\frac{2\pi r_i(\varphi)}{\lambda}}, \quad (2)$$

where w_i defines the magnitude and phase of the i-th element. r_i is the distance between the i-th element position and the point of observation in the far field w.r.t. the DOA. The overall array radiation pattern C_{array} is defined as:

$$C_{\mathrm{array}} = C_{\mathrm{E}} \cdot AF, \quad (3)$$

where C_{E} is the radiation pattern of a single antenna element. E.g., the radiation pattern of a half-wave dipole aligned in ϑ direction is described by [7]:

$$C_{\mathrm{dipol}}(\varphi, \vartheta) = \frac{\cos\left(\frac{\pi}{2}\cos\vartheta\right)}{\sin\vartheta}, \quad (4)$$

where in a spherical coordinate system φ is the azimuth angle and ϑ is the elevation angle. Combining (2), (3)

and (4) the array radiation pattern of multiple dipoles is described by:

$$C_{\text{array}} = \frac{\cos\left(\frac{\pi}{2}\cos\vartheta\right)}{\sin\vartheta}\sum_{i=0}^{n-1} w_i e^{-j\frac{2\pi r_i(\varphi)}{\lambda}}. \quad (5)$$

In Figure 2 the antenna patterns 'blue' and 'red' for the corresponding dipole pairs with $w_1 = w_2 = 1$ are generated. The approach features four dipoles to generate two orthogonal antenna patterns. In Figure 2c the resulting field strength difference for different DOAs is shown. The assumption in [4] was, all dipoles are fed by the same RF signal, so $w_1 = w_2 = 1$ and the current inside the dipoles I_{e} is in-phase at all dipoles. Feeding the dipoles with individual phases α_i, allows for variation of the antenna pattern. The complex weight w inside the AF is used to realize different antenna beams. Therefore, the number of dipoles may be minimized by using the same physical dipoles to form multiple antenna patterns. Feeding with different phases is described by the complex weight w_i expressed as

$$w_i(\alpha_i) = \hat{w} \cdot e^{j\alpha_i}, \quad (6)$$

where α is the phase shift of the i-th array element. The phase shift between two elements is given by:

$$\phi_{ij} = \alpha_i - \alpha_j. \quad (7)$$

The resulting antenna pattern at 868 MHz for feeding the blue dipoles in-phase, i.e. $\phi_{12} = 0$, is depicted in Figure 2b by the blue dashed pattern. The green dashed dotted pattern in Figure 2b illustrates the result of feeding the antennas out-of-phase, i.e. $\phi_{12} = \pi$. The in-phase and out-of-phase feeds basically represent the arrays eigenmodes [8]. These are the two fundamental modes of radiation for a two-element array. They read $1/\sqrt{2}\,(\,1\;1\,)^{\text{T}}$ for the in-phase feed (even mode) and $1/\sqrt{2}\,(\,1\;-1\,)^{\text{T}}$ for the out-of-phase feed (odd mode). All possible feeds can be considered a linear combination of the eigenmodes. Due to their orthogonality, the radiation patterns corresponding to the eigenmodes are mutually decoupled.

4 Antenna Design and Results

For mechanical reasons and application requirements it is beneficial to have a ground plane. Hence, for the prototype design monopoles were chosen as array elements. Following [9] with methods of imaging, monopoles on an infinite ground plane are described as dipoles with some limitations. For monopoles with a finite ground plane the size of the ground plane influences the radiation characteristics due to the edge diffraction. Edge diffraction induces undesired side-lobes in the antenna pattern. Simulations reveal that an elliptical ground plane adds additional lobes, thus, a circular-plane was chosen. The size is mainly limited by the lower frequency and has roughly the minimal possible diameter of one λ_0 [10], where λ_0 is a free space wavelength. The initial monopole length is assumed to measure $0.25\lambda_0$ in length.

Figure 3: The antenna prototype

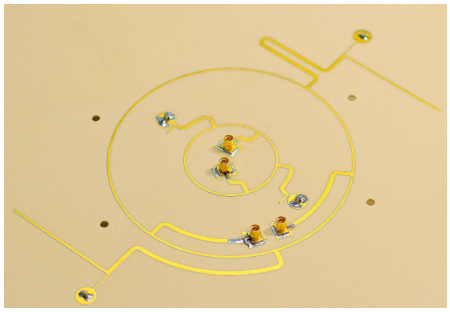

Figure 4: Close-up of the back-side of the antenna prototype, including matching network and 180° hybrid coupler.

In the following subsections the geometrical arrangement of the antenna elements to each other are discussed as well as the minimization of coupling between the antenna elements. The implemented prototype dual band antenna is shown in Fig. 3.

4.1 Geometrical Arrangement

For dual-band operation, two arrays are arranged on a single ground plane, as depicted in Figure 2a. Each array comprises two monopoles. Coupling between the monopoles affects the radiation characteristics and therefore the DOA estimation accuracy, which relies on a proper pattern. As seen in Figure 2b for an array operating at 868 MHz, this effect is particularly pronounced for the even-mode pattern (red elements, $\phi_{12} = 0$), which displays side-lobes due to the presence of the array operating at 2.4 GHz (black elements). Similar

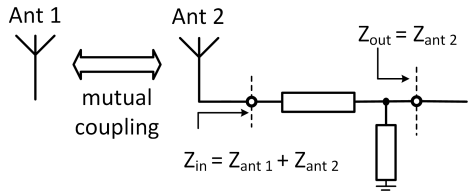

Figure 5: Antenna decoupling applying a two-stage network.

behavior occurs at 2.4 GHz, as revealed by further simulations. In addition to the pattern distortion, the resonant frequency of the reflection coefficient at the antenna feed points is shifted. Beyond the eight-like pattern, the antenna design focuses on the decoupling of the elements.

4.2 Reduction of Coupling between Elements

To migrate coupling between elements a two-stage approach is pursued. Firstly, the shape of the monopoles themselves is optimized. Secondly, the matching of the single elements is optimized to minimize coupling.

4.2.1 Mechanical arrangement for minimized coupling

By varying the spacing, the ratio of the input power and the transferred power between elements changes. The coupling alters depending on the particular frequency, which can be considered as the influence of mutual impedance. As a conclusion of the analysis of mutual impedance in [11] the antennas in a small separation configuration need to be orthogonally aligned to each other to have a minimal mutual coupling. This can also be interpreted as polarization decoupling.

A folding by 90 degrees for the 868 MHz antenna elements show sufficient results with minimized side-lobes for the even-mode pattern. For 2.4 GHz the side-lobes are also reduced, but still present. The simulations show slightly better characteristics for straight monopoles at 2.4 GHz and folded monopoles at 868 MHz than reversed. In addition, the folded monopoles at 868 MHz are chosen due to higher expected mechanical stability. In Figure 3 the orthogonal arrangement of the folded 868 MHz and unfolded 2.4 GHz elements are illustrated. In fact by simple geometrical separation it is not possible to produce optimal pattern without side-lobes for both frequencies. Furthermore, designing the specified pattern for both frequencies requires compensation of mutual coupling.

Antenna	f in MHz	Mag in dB
1	**868**	-32.36
	2450	-1.63
2	868	-0.07
	2450	-24.11

Table 1: Magnitude of reflection coefficient of antenna elements. The frequency of operation is bold.

4.2.2 Pattern optimization through matching

Figure 5 illustrates two antenna elements with mutual coupling. If antenna element 1 is excited, a portion of the radiated energy appears at the radiation pattern of antenna element 2. An additional mean is crucial to minimize the interaction between each element. Due to a certain matching of the antenna element feed-points the portion of the radiated power can be significantly reduced at the other antenna element. Assuming two different operation frequencies $f_{\mathrm{c}1}$ and $f_{\mathrm{c}2}$ for both antennas, the single antenna is matched to its resonance frequency with a low reflection coefficient $\Gamma_{\mathrm{in}} \approx 0$. The matching for the non resonance frequency is optimized to full-fill $\Gamma_{\mathrm{in}} \approx \pm 1$, leading for the antenna with resonance frequency $f_{\mathrm{c}1}$ to the conditions $\Gamma_{\mathrm{in}}(f_{\mathrm{c}1}) = 0$ and $\Gamma_{\mathrm{in}}(f_{\mathrm{c}2}) = \pm 1$. An example is depicted in Figure 5, with antenna element 2 using a two-stage network to match at the resonance frequency and simultaneously reflecting the power received at operation frequency of antenna element 1. Both antennas consist of a two-stage network with a transformer and open or short-circuited stub. In Figure 4 the feed-network is presented. In Table 1 the magnitude of the reflection coefficient of both antennas at the relevant frequencies is presented.

4.3 Feed Network

The purpose of the feed network is to feed the radiating array elements at the operable bands. A $180°$ hybrid coupler is choosen to excite the array elements with equal amplitudes and phases of $\phi = 0°$ and $\phi = \pi$. The inner coupler operates at 2.4 GHz and the outer coupler operates at 868 MHz. Trombone-like delay line (cf. Figure 4) is required to obtain the phase relation.

4.4 Results

The prototypes were fabricated on a substrate with relative permittivity of $\varepsilon_{\mathrm{r}} = 4.08$ at 868 MHz and $\varepsilon_{\mathrm{r}} = 4.06$ at 2.4 GHz [12]. Figure 6 shows the radiation pattern obtained from measurements of the 868 MHz array and the 2.4 GHz array in comparison to the results

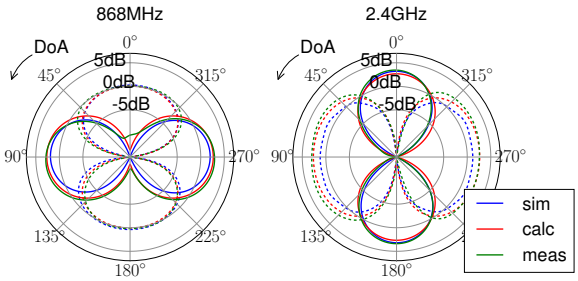

Figure 6: Comparison of analytically calculated antenna pattern by dipoles, simulated antenna pattern of monopoles in HFSS and measured antenna pattern in an anechoic chamber for both frequencies.

obtained from calculations and simulations. The eight-like patterns are clearly pronounced without appearance of side-lobes. Calculations, simulations and measurements prove to be in good agreement.

5 Conclusion

In this paper, a dual frequency array prototype providing an eight-like pattern for DOA measurements has been proposed. Applying an in-phase and out-of-phase feeding, the antenna pattern shape is achieved with two monopoles per frequency, only. The spatial distribution of the elements was been optimized for the small separation configuration. Ultimately, the pattern zeros have been accomplished with a matching an decoupling network. The couplers of both arrays are arranged to provide the proper feed signals to the elements, as depicted in Figure 4. Due to reduced coupling, the resulting pattern characteristics show negligible side-lobes. Therefore, the proposed antenna array is suitable for precise field strength-based DOA estimation in two frequency bands. Compared to phase-based approaches this allows for DOA estimation with receivers at low synchronization level providing no phase coherent sampling of two antenna ports. Hence, the proposed RSS-DOA antenna represents an excellent alternative to phase-based arrays especially for energy-constrained and low-cost sensor networks.

Acknowledgements

This work is supported by German Science Foundation DFG under Grant FOR 1508, Research Unit BATS. Furthermore, the authors are grateful to their colleagues Lucila Patino-Studencki, Alexander Popugaev and Jörg Robert for their helpful comments.

References

[1] Mainwaring, A., Culler, D., Polastre, J., Szewczyk, R., Anderson, J., 2002, Wireless sensor networks for habitat monitoring, *Proceedings of the 1st ACM international workshop on Wireless sensor networks and applications*. pp. 88–97.

[2] Hierold, M., Ripperger, S., Mayer, F., Weigel, R., Koelpin, A., 2015, System design for encounter detection of distributed wireless sensors, *German Microwave conference 2015*. pp. 382–385.

[3] Hartmann, M., Nowak, T., Pfadenhauser, O., Thielecke, J., Heuberger, A., 2016, A grid-based filter for tracking bats applying field strength measurements, *Proceedings of the 2016 IEEE/IFIP Wireless on-demand network systems and services conference*. pp. 184–191.

[4] Hartmann, M., Pfadenhauser, O., Patino-Studencka, L., Troeger, H., Heuberger, A., Thielecke, J., 2015, Antenna pattern optimization for a RSSI-based direction of arrival localization system, *Proceedings on the ION 2015 pacific PNT meeting*. pp. 429–433.

[5] Giorgetti, G., Maddio, S., Cidronali, A., Gupta, S. K. S., Manes, G., 2009 Switched beam antenna design principles for Angle of Arrival estimation, *European Wireless technology conference EuWIT 2009*. pp. 5–8.

[6] Balanis Constantine, A., 1997, Antenna theory: analysis and design. *John Wiley & Sons, Inc.*

[7] Chang, K., 2003, Handbook of RF/Microwave components and engineering *Wiley*

[8] Vomer, C., Weber, J., Stephan, R., Blau, K., Hein, M.A., 2008, An eigen-analysis of compact antenna arrays and its application to port decoupling, *Journal IEEE Transactions on Antennas and Propagation* Vol. **56**, pp. 360–370.

[9] Weiner, M.M., 2003, Monopole antennas, *CRC Press*

[10] Milligan, T. A., 2005, Modern antenna design, *Wiley-IEEE Press*

[11] Garg, R., 2001, Microstrip antenna design handbook, *Artech House*

[12] Panasonic corporation, 2014, Megtron 4 (L) aminate (R)-5725, *PANASONIC Corporation*